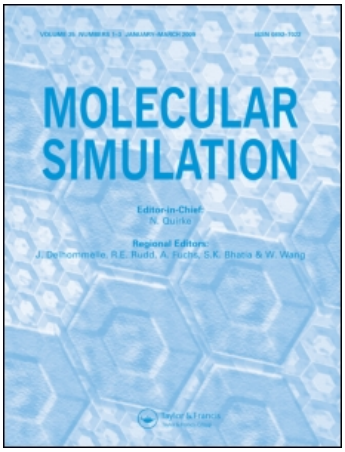


**Molecular Simulation**
Publication details, including instructions for authors and subscription information:
http://www.informaworld.com/smpp/title~content=t713644482

# Theoretical studies on the interaction of guanine riboswitch with guanine and its closest analogues

Baoping Ling[a]; Rui Zhang[b]; Zhiguo Wang[b]; Lihua Dong[b]; Yongjun Liu[ab]; Changqiao Zhang[a]; Chengbu Liu[a]
[a] School of Chemistry and Chemical Engineering, Shandong University, Jinan, Shandong, P.R. China [b] Northwest Institute of Plateau Biology, Chinese Academy of Sciences, Xining, Qinghai, P.R. China

Online publication date: 02 November 2010

**To cite this Article** Ling, Baoping , Zhang, Rui , Wang, Zhiguo , Dong, Lihua , Liu, Yongjun , Zhang, Changqiao and Liu, Chengbu(2010) 'Theoretical studies on the interaction of guanine riboswitch with guanine and its closest analogues', Molecular Simulation, 36: 12, 929 — 938
**To link to this Article: DOI:** 10.1080/08927022.2010.492833
**URL:** http://dx.doi.org/10.1080/08927022.2010.492833

*Molecular Simulation*
Vol. 36, No. 12, October 2010, 929–938

Taylor & Francis
Taylor & Francis Group

# Theoretical studies on the interaction of guanine riboswitch with guanine and its closest analogues

Baoping Ling[a], Rui Zhang[b], Zhiguo Wang[b], Lihua Dong[b], Yongjun Liu[ab]*, Changqiao Zhang[a] and Chengbu Liu[a]

[a]*School of Chemistry and Chemical Engineering, Shandong University, Jinan, Shandong 250100, P.R. China;* [b]*Northwest Institute of Plateau Biology, Chinese Academy of Sciences, Xining, Qinghai 810001, P.R. China*

(*Received 19 October 2009; final version received 9 May 2010*)

Experimental studies (M. Mandal, B. Boese, J.E. Barrick, W.C. Winkler and R.R. Breaker, *Riboswitches control fundamental biochemical pathways in bacillus subtilis and other bacteria*, Cell 113 (2003), pp. 577–586) demonstrated that, besides recognising guanine with high specificity, guanine riboswitch could also bind guanine analogues, but the alteration of every functionalised position on the guanine heterocycle could cause a substantial loss of binding affinity. To investigate the nature of guanine riboswitch recognising metabolites, molecular docking and molecular dynamics simulation were carried out on diverse guanine analogues. The calculation results reveal that (1) most guanine analogues could bind to guanine riboswitch at the same binding pocket, with identical orientations and dissimilar binding energies, which is related to the positions of the functional groups; (2) the two tautomers of xanthine adopt different binding modes, and the enol-tautomer shows similar binding mode and affinity of hypoxanthine, which agrees well with the experimental results and (3) the riboswitch could form stable complexes with guanine analogues by hydrogen bonding contacts with U51 and C74. Particularly, U51 plays an important role in stabilising the complexes.

**Keywords:** guanine; guanine riboswitch; docking; molecular dynamics; binding energy



## 1. Introduction

Riboswitches are gene control elements located in 5′-untranslated regions of certain bacterial mRNA [1]. They are capable of binding specific small molecular metabolites to regulate gene expression through conformational changes [2]. Most riboswitches are composed of two distinct domains: an aptamer domain and an expression platform domain. The aptamer domain can selectively bind metabolites and transmit message to the downstream expression platform domain, which brings about structural changes to modulate gene expression [3]. In recent years, over 20 types of riboswitches have been identified to regulate expression of a diverse set of genes at transcriptional and translational levels, which recognise small molecular metabolites including amino acid [4,5], vitamin [6], purine [7,8], metal ions [9] and so on.

Up to now, there are four classes of identified purine riboswitches. Three of them have conserved sequences and similar secondary structures, yet they could discriminate adenine, guanine and 2′-deoxyguanosine with high selectivity, respectively [10]. The recent studies of Edwards and Batey [11] revealed that, when uracil at position 51 was mutated to cytosine, the recognising specificity of guanine riboswitch could convert from guanine to 2′-deoxyguanosine. While the mutation was conducted at position 74 from cytosine to uracil, the specificity would switch from guanine to adenine [12]. However, when some conserved nucleotides were mutated, the riboswitch kept recognising its original ligands. For example, the guanine riboswitch still specifically recognised hypoxanthine (HPA) in spite of some conserved nucleotides being mutated [13]. It can be deduced that the key nucleotides being responsible for specificity would be those interacting directly with metabolites in the binding pocket. These key nucleotides often form Watson–Crick base pair interactions with the ligands, and other nucleotides in the pocket form additional hydrogen bonds with the ligands to shape three-way junctions [13]. Therefore, only some key mutations are required in the general conserved secondary structures for converting the specificity of the riboswitch [10]. Gilbert's experiment [12] demonstrated that purine riboswitch not only recognises some purine ligands, but also recognises its closest analogues.

The binding affinities of the riboswitches are greatly affected by sequence context of the aptamer domain, and they would change significantly when the less conserved nucleotides in the core of aptamer domain are mutated. The binding assays on 2-aminopurine demonstrated that the introduction of different nucleotides at positions 24, 48 or 73 of purine riboswitch would cause a remarkable decrease in the binding affinity [14]. Besides the structure

*Corresponding author. Email: yongjunliu_1@sdu.edu.cn

ISSN 0892-7022 print/ISSN 1029-0435 online

DOI: 10.1080/08927022.2010.492833
http://www.informaworld.com

of riboswitch itself, the structures and functional groups of ligands also play an important role in binding affinity. The alteration of the functional groups often results in a substantial change in the binding affinity.

Experimentally, the binding affinities of the ligands for a given riboswitch are examined by measuring their dissociation constants ($K_D$). Mandal's experiments [15] revealed that guanine riboswitch could discriminate guanine, HPA, xanthine and adenine. The $K_D$ value of guanine was $\leq 5$ nM while that of adenine was $>300{,}000$ nM. The $K_D$ values of HPA and xanthine were about 50 nM. The different dissociation constants of other analogues indicated that the alteration of every functionalised position on guanine heterocycle could cause a substantial loss of the binding affinity. However, how the functional groups will affect the binding mode and affinity is still unclear, and the estimation of dissociation constant is built upon experiments. Particularly, the determination of- dissociation constant with low value (like $<2$ nM) is still a problem due to insufficient levels of signal for measuring.

Molecular docking and molecular dynamics (MD) simulations have been extensively applied in the study of biological macromolecules [16–19]. Recently, the simulations on riboswitches draw much attention [20,21]. In the previous paper, we employed molecular docking and MD simulations to study the binding of mutated guanine riboswitch with modified pyrimidines and purines [22]. In this paper, we will investigate the interactions of guanine riboswitch with structural diverse guanine analogues, with the aim to understand how the functional groups and methyl substitution will affect the binding mode and affinity, and get an insight into the nature of guanine riboswitch for recognising metabolites.



## 2. Methods

For comparison, we selected some ligands from Mandal's experiment [15]. These ligands carry different functional groups or substituents such as oxygen, sulphur, bromine or methyl (Figure 1). In addition, in order to explore the influence of steric hindrance on the binding affinity, we designed some ligands, namely, 1-methylguanine (1MGu), 2-methyl-6-oxypurine (2MPu), 2-amino-6-methylpurine (6MPu), 8MPu and 9MGu.

The guanine riboswitch was taken from the Brookhaven Protein Data Bank (www.rcsb.org), PDB code of 1U8D with resolution of 1.95 Å, and the 3D structure of riboswitch bound to HPA is shown in Figure 2.

All the structures of ligands were fully optimised using Gaussian 03 program [23] at B3LYP/6-31 g (d, p) level. The labels of all the analogues were consistent with those of guanine (Figure 1). Before docking, all the substances other than receptor (riboswitch) were removed from the crystal structure, then polar hydrogen atoms were added, at last Kollman atom charge was added and assigned to the receptor.

### 2.1 Parameters set-up for molecular docking

AutoDock program [24] is based on the empirical binding free energy function and Lamarckian genetic algorithm [25–28]. We applied AutoDock version 4.0 to perform molecular docking. When docking, the riboswitch was treated as rigid while the ligand was allowed torsional flexibility. The grid size was set to $80 \times 80 \times 80$ points by AutoGrid with a grid-point spacing of 0.375 Å. The centroid of four nucleotides, U22, U47, U51 and C74, served as the centre of grid box. Initially, we used a population size of 150, a maximum number of $2.5 \times 10^7$ energy evaluations, a maximum number of generations of 27,000, a crossover rate of 0.8 and a mutation rate of 0.02. The pseudo Solis & Wets method was applied for local search with a maximum number of 300 iterations. The local search probability for an individual was 0.06 and the maximum number of consecutive successes or failures was 4 [29–31]. Fifty independent docking runs were carried out for each ligand, the docking results less than 0.5 Å in positional root mean square deviation (RMSD) were clustered, and the best conformation with the lowest energy and the greatest number of members in cluster were adopted as the initial structure for the following MD simulation.

### 2.2 Parameters set-up for MD simulation

The starting structure was solvated in an $81 \times 81 \times 81$ Å TIP3P water box with periodic boundary condition, 67 water molecules were replaced randomly by potassium cations to maintain system neutralisation. MD simulations were performed by using GROMACS 4.0.2 program [32] in AMBER99 force field [33–36] in NTP ensemble. During simulations, the pressure was controlled at $1.01 \times 10^5$ Pa using Berendsen pressure coupling method with coupling coefficient of 0.5 ps. Similarly, the temperature was maintained at 300 K by Berendsen temperature coupling method with a coefficient of 0.1 ps. Long-range electrostatic interactions were treated with particle-mesh Ewald algorithm, a 10 Å cut-off for coulomb interaction, a 14 Å cut-off for van der Waals interaction, and all bond lengths including hydrogen atoms were constrained using LINCS algorithm [37].

Firstly, the system was subjected to 8000 steps of steepest descent energy minimisation; followed by 100 ps position restrained dynamics with a 1000-kJ/(mol nm$^2$) harmonic distance constraint fixed riboswitch and ligand; subsequently, all the restraints were removed, the MD simulations were continued for 10 ns, wherein the time step was set as 2 fs and the dynamics trajectories were saved every 2 ps for analysis.

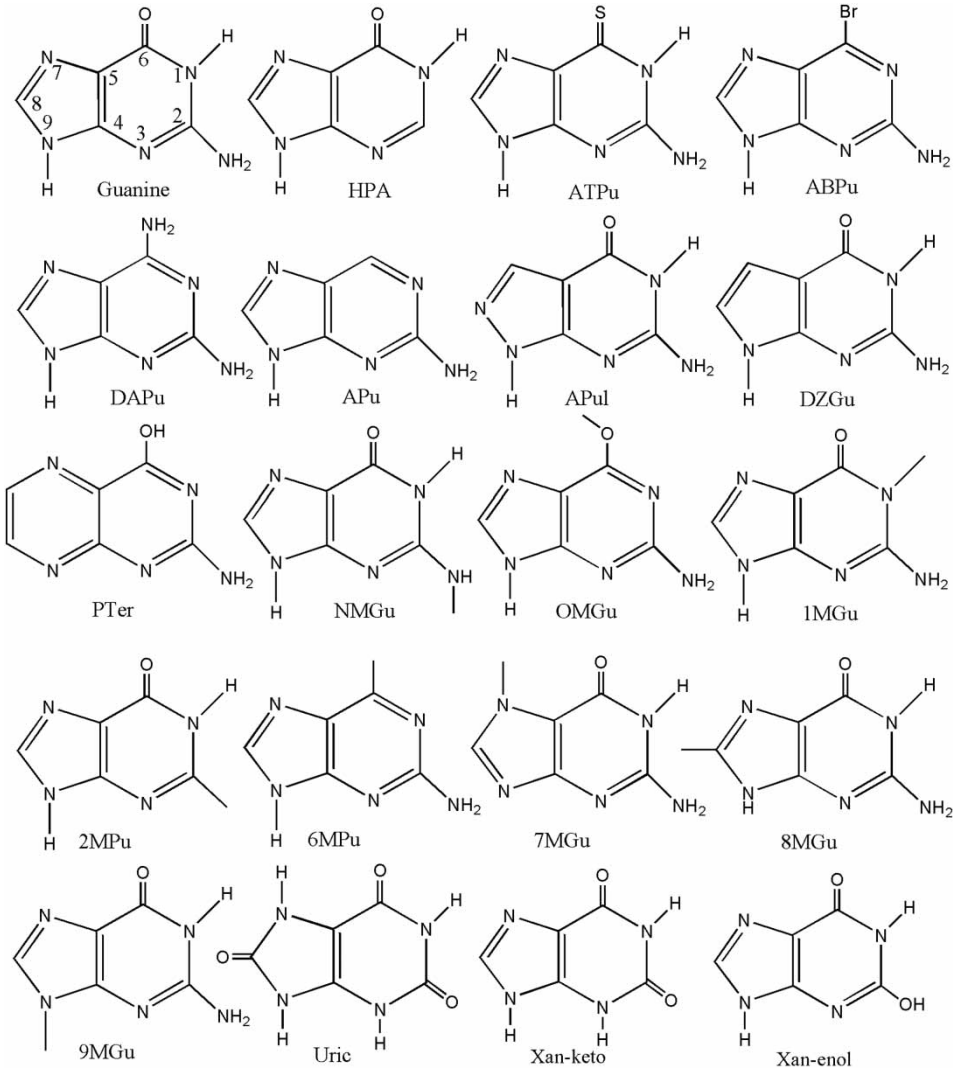


Figure 1. Chemical structures of guanine and its analogues used for docking.

## 3. Results and discussion

### *3.1 Docking*

At first, molecular docking was applied to guanine and HPA. All molecular figures were generated with *chimera* [38]. The docking results are shown in Figure 3, in which two ligands located in the same binding pocket consisted of U22, U47, U51 and C74, with the same orientation. Both guanine and HPA form hydrogen bonds with U51 and C74. At the same time, N7 in the five-member ring of ligands forms one hydrogen bond with the hydroxyl of U22. The superimposition of the docking conformation of HPA and its crystal structure is also shown in Figure 3, in which the two structures are almost superimposed together, suggesting that the docking conformation agrees well with the crystal structure [39,40]. Therefore, we used the same docking procedure to study other ligands. We will discuss the interactions according to the following aspects.

#### *3.1.1 Orientations of the ligands in the binding pocket*

Figure 4 shows the docking results of 2-amino-6-thiopurine (ATPu), 2-amino-6-bromopurine (ABPu), 2,6-diamino-purine (DAPu) and 2-amino-purine (APu). These four ligands contain different substituents at 6-position, but they display the same orientations and binding pocket as that of guanine, which means that the substituents at 6-position cause a negligible influence on the binding mode of the ligands.

Figure 5 shows the docking conformations of allopurinol (APul) and 7-deazaguanine (DZGu). In APul, nitrogen atom at 7-position is replaced by carbon and the carbon atom at 8-position is substituted by nitrogen. Whereas in DZGu, only one nitrogen atom at 7-position is replaced by carbon. As shown in Figure 5, APul and DZGu still have the same orientations as that of guanine. Therefore, changes on the five-member ring still cause insignificant influence on the binding of the ligands.

Figure 2. The 3D structure of guanine riboswitch bound to HPA (PDB ID: 1U8D). The base A is shown in red, U is shown in cyan, G is shown in green, C is shown in yellow and HPA is shown in blue (colour online).

We introduced methyl at different positions to study the influence of steric hindrance on the binding modes. In $N^2$-MGu (NMGu) and $O^6$-MGu (OMGu), methyl is introduced to amino group at 2-position or to carbonyl at 6-position, respectively. In 1MGu, 2MPu, 6MPu and 8MGu, methyl is introduced at 1-, 2-, 6- and 8-position, respectively. Their docking results are shown in Figures 6 and 7. One can see that the orientations of the ligands remain the same. However, when methyl is introduced at 7- or 9-position, such as in 7MGu and 9MGu (Figure 8), their orientations change obviously. It is because the spaces near 7- or 9-position of the ligands in the binding pocket are too small to accommodate the methyl group.

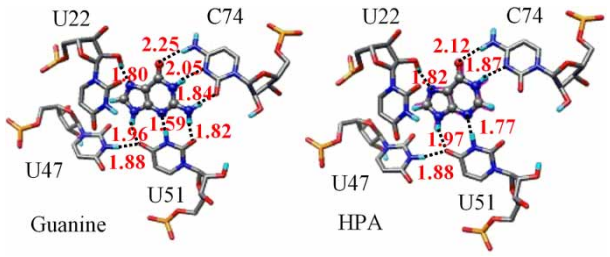


Figure 3. Docking conformations of guanine riboswitch complexed with guanine and HPA. The dotted lines represent hydrogen bonds. The data are bond lengths in Å.

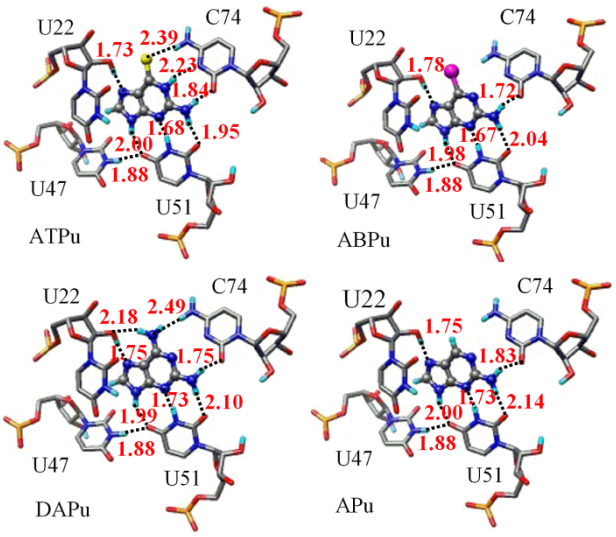


Figure 4. Docking conformations of guanine riboswitch complexed with ATPu, ABPu, DAPu and APu, respectively. The dotted lines represent hydrogen bonds. The data are bond lengths in Å.

We also studied uric acid (Uric) and pterin (PTer). In Uric, carbonyl is introduced at 2- and 8-position of guanine; in PTer, the five-member ring is replaced by a six-member ring. Their docking results are shown in Figure 6, and no obvious changes are observed in the orientation of the ligands.

### 3.1.2 *Influence of functional groups on the binding affinity*

The experiment by Mandal et al. [15] demonstrated that the alteration of every functionalised position on guanine heterocycle could cause a substantial loss of binding affinity. Accordingly, we calculated the binding energies of all the analogues.

The binding energies of the docking conformations with lowest energy are shown in Table 1. It can be seen

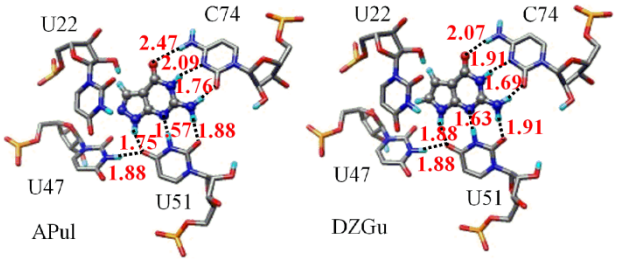


Figure 5. Docking conformations of guanine riboswitch bound APul and DZGu. The dotted lines represent hydrogen bonds. The data are bond lengths in Å.

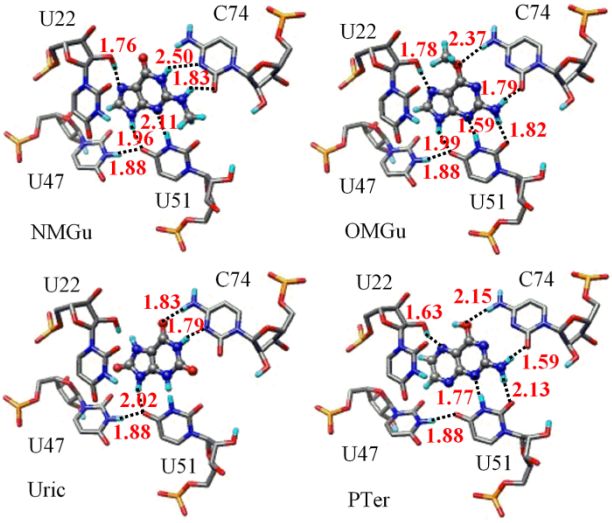


Figure 6. Docking conformations of guanine riboswitch bound NMGu, OMGu, Uric and PTer, respectively. The dotted lines represent hydrogen bonds, and the data are bond lengths in Å.

that the binding energies of the ligands are greatly different from each other. The binding energy of ABPu is −9.2 kcal/mol, while that of Uric is only −4.8 kcal/mol.

Molecular docking only gives the approximate value of the binding energy. For more accurately comparing the changing tendency of binding affinities, we employed cluster model to calculate the binding energies. In our calculation, the ligand and its surrounding nucleobases were treated as the cluster model. The structure of the ligand was fully optimised while the surrounding nucleobases were fixed. The binding energies ($\Delta E$), calculated at B3LYP/6-31 g (d, p) level by using Gaussian 03 program,

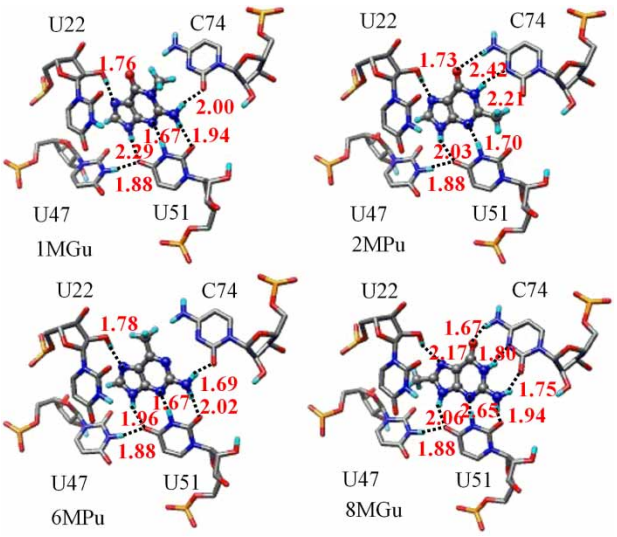


Figure 7. Docking conformations of guanine riboswitch bound 1MGu, 2MPu, 6MPu and 8MGu, respectively. The dotted lines represent hydrogen bonds, and the data are bond lengths in Å.

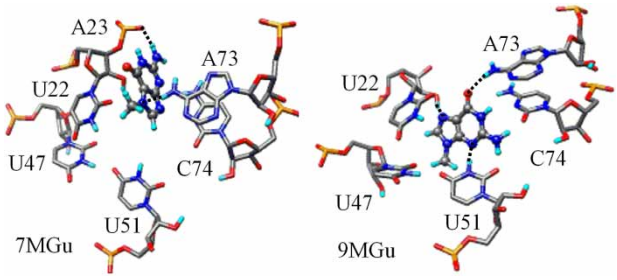


Figure 8. Docking conformations of guanine riboswitch bound 7 and 9MGu, respectively. The dotted lines represent hydrogen bonds, and the data are bond lengths in Å.

are listed in Table 1. We can see that the absolute values of the binding energies from docking are different from those of *ab initio* calculation, but their tendency is similar on the whole, especially the changing tendency of *ab initio* calculation agrees well with that of experiment.

The guanine riboswitch could recognise guanine from adenine, and the oxygen atom at 6-position is an important determinant for molecular recognition [15]. The calculated results reveal that, when the oxygen atom of guanine is substituted by sulphur, the binding mode does not change (Figure 4). But the strength of hydrogen bond between sulphur atom and nucleobase is weakened, which results in the decrease in the binding affinity.

When the oxygen atom of guanine at 6-position is replaced by bromine, amino group or hydrogen such as in

Table 1. Diverse energies (kcal/mol) of guanine riboswitch complexes with the ligands.

| Ligands | Binding energy[a] | $\Delta E$[b] | $\Delta G_{exp}$[c] | Log $K_{D,exp}$ (M)[d] |
|---|---|---|---|---|
| Guanine | −7.3 | −58.0 | −11.3 | ≤ −8.4 |
| HPA | −6.1 | −47.4 | −10.0 | −7.3 |
| ATPu | −9.1 | −55.4 | −8.2 | −6.0 |
| ABPu | −9.2 | −42.0 | −8.9 | −6.5 |
| DAPu | −8.3 | −42.3 | −6.8 | −5.0 |
| APu | −8.1 | −38.5 | −6.8 | −5.0 |
| DZGu | −6.6 | −50.7 | −8.2 | −6.0 |
| APul | −6.7 | −48.4 | −5.5 | < −4.0 |
| NMGu | −7.5 | −50.0 | −9.6 | −7.0 |
| OMGu | −8.8 | −38.8 | −8.9 | −6.5 |
| Uric | −4.8 | −32.6 | −5.5 | −4 |
| PTer | −7.6 | −28.8 | −4.8 | < −3.5 |
| Xan (enol) | −6.3 | −47.0 | −10.0 | −7.3 |
| 1MGu | −6.0 | −46.9 | | |
| 2MPu | −6.6 | −46.5 | | |
| 6MPu | −8.8 | −40.3 | | |
| 7MGu | | | −5.9 | −4.3 |
| 8MGu | −5.6 | −56.1 | | |
| 9MGu | | | | |

[a] The binding energies are calculated by molecular docking. [b] $\Delta E$ is calculated at b3lyp/6-31 g (d, p) level, where $\Delta E = E_{complex} - (E_{base} + E_{ligand})$. [c] $\Delta G_{exp}$ is calculated according to the formula: $\Delta G = RT\ln K_D$ [12], where $K_D$ values are from reference [15]. [d] Log $K_{D,exp}$ data are from reference [15].

ABPu, DAPu and APu, the number of hydrogen bonds between the ligands and C74 decreases, but they still form three hydrogen bonds with U51, and the hydrogen bond between nitrogen atom at 7-position and hydroxyl of U22 still exists. From the energy point of view, the binding energies ($\Delta E$) decrease from $-55.4$ to $-38.5$ kcal/mol, displaying similar tendency to those of experiment (values of $\Delta G$ and log $K_D$ in Table 1). One can see that, although these ligands have the same orientations in the binding pocket, their binding affinities are very different.

Our previous work verified that the amino group at 2-position of pyridine could facilitate the ligand binding [22], for there are superfluous space in the binding pocket to accommodate the exocyclic amino group, and the amino group could form hydrogen bonds with U51 and C74. Compared with guanine, HPA lacks one amino group at 2-postion and forms less intermolecular hydrogen bonds than guanine, therefore, its binding affinity decreases (The calculated binding energies of HPA and guanine are $-47.4$ and $-58.0$ kcal/mol, respectively). The removal of amino group causes a 10.6 kcal/mol loss of binding affinity, which is consistent with the changing tendency of experimental results of Batey et al. [39].

When guanine has abolished the oxygen atom at 6-position and becomes APu, the calculated binding energy is 19.5 kcal/mol higher than that of guanine ($-38.5$ vs. $-58.0$ kcal/mol), i.e. the removal of carbonyl group at 6-position causes a 19.5 kcal/mol loss of binding affinity.

Modification of the five-member ring also affects the binding energy. The nitrogen atom at 7-position of guanine can form strong hydrogen bond with U22. When the nitrogen atom is substituted by carbon atom, such as in APul and DZGu, the original hydrogen bond at 7-position disappears and the binding energies decrease noticeably (Table 1).

The introductions of carbonyl at 2- and 8-position of guanine can also affect the binding energy. For example, the binding energy of Uric is only $-32.6$ kcal/mol. Similarly, when the five-member ring of purine changes to six-member ring and the carbonyl at 6-position is replaced by hydroxyl (such as PTer), the binding energy decreases to $-28.8$ kcal/mol.

In a word, the oxygen atom at 6-position and amino group at 2-position of guanine could facilitate the binding of the ligands. The weakness or loss of hydrogen bonds is responsible for the decrease in binding energy.

### 3.1.3 *Influence of steric hindrance on the binding affinity*

Experimental results revealed that methyl at 7-position of guanine (7MGu) could weaken the binding. The log $K_D$ of 7MGu is only $-4.3$ M. However, the methyl group on the amino group at 2-position (NMGu) or on the carbonyl at 6-position (OMGu) only results in a minor decrease in the binding energies, with the log $K_D$ of $-7$ and $-6.5$ M, respectively [15]. Our docking calculation shows that 7MGu could not enter the original binding pocket due to the steric effect of methyl group but binds in another pocket constituted by nucleobases U22, A23 and A73, as shown in Figure 8. Whereas NMGu and OMGu still bind in the original binding pocket (Figure 6). The calculated binding energy of NMGu and OMGu at B3LYP/6-31 g (d, p) level is $-50.0$ and $-38.8$ kcal/mol, respectively, which are higher than that of guanine ($-58.0$ kcal/mol).

To study the influence of steric effect on the binding affinities, we introduced methyl groups at different positions of guanine, such as in 1MGu, 2MPu, 6MPu, 8MGu and 9MGu (Figure 1). The docking results show that the methyl group at 1-, 2-, 6- and 8-position could not affect the orientations of the ligands (Figure 7). But the presence of methyl groups causes some changes in the binding modes. The position and number of hydrogen bonds changed, and their binding affinities decreased compared with guanine. The binding energies of 1MGu, 2MPu and 6MPu are all larger than $-47.0$ kcal/mol. These results suggest that the purine riboswitch could recognise ligands with small functional groups at 1-, 2-, 6- and 8-position.

We also notice that the ligands bearing diverse functional groups at 2-position, such as in HPA, NMGu and 2MPu, correspond to the similar binding energies ($\sim -47.0$ kcal/mol) which are a little higher than that of guanine. It implies that the amino group at 2-position of guanine could facilitate the ligand binding, but the alteration of functional groups at 2-position of other ligands does not affect the binding energies.

The docking on 9MGu reveals that the methyl on 9-position causes a great steric hindrance; 9MGu binds in another pocket constituted by U22, U51 and A73, as shown in Figure 8.

Accordingly, the introduction of methyl group to guanine at 7- and 9-position could seriously affect the binding modes and affinities with the binding pocket changed. But for the introduction at 1-, 2-, 6- and 8-position, the ligands still bind in the original pocket, only the binding affinities are weakened.

### 3.1.4 *The orientation and binding mode of xanthine*

The experiment verified that the binding affinity of xanthine (Xan) was almost equal to that of HPA, and the $K_D$ of Xan was about 50 nM [15]. To compare the difference between Xan and HPA upon binding to riboswitch, we performed molecular docking on Xan. The docking result indicates that the orientation of the keto-tautomer of Xan (Xan-keto) is clearly different from that of HPA. Although Xan-keto binds in the same binding pocket, its binding mode is different from that of HPA (Figure 9). However, we used the enol-tautomer of Xan (Xan-enol) to perform docking and the obtained

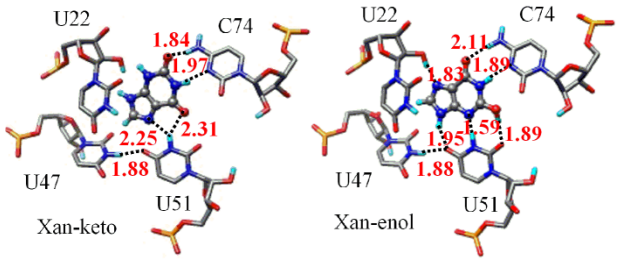


Figure 9. Docking conformations of guanine riboswitch bound Xan tautomer. The dotted lines represent hydrogen bonds, and the data are bond lengths in Å.

orientation and binding mode are totally the same as those of HPA and guanine, which agrees well with the crystal structure solved by Gilbert [41].

The reason of Xan-keto using different binding modes is probably due to the electrostatic repulsion of NH at 3-position with the NH of U51, and carbonyl at 2-position with the two carbonyls of U51 and C74. Thus Xan-keto could not form hydrogen bonds with U51 and C74. However, Xan-enol has a similar framework as HPA and contains one additional hydroxyl at 2-position, which forms additional hydrogen bond with the carbonyl of U51. The additional hydrogen bond enhances the binding of the ligand. The binding energy of Xan-enol calculated at B3LYP/6-31 g (d, p) level is −47.0 kcal/mol, which is comparable with that of HPA (−47.4 kcal/mol). It agrees well with Mandal's experiment (HPA and Xan exhibited same binding affinity and $K_D$ values) [15].

In summary, except 7MGu and 9MGu which cannot be docked into the original binding pocket, all the other ligands bearing different functional groups are bound in the same pocket. The superposition of six selected ligands in the binding pocket is shown in Figure 10. One can see that the backbones of the six ligands are almost superimposed, except a slight incline of Uric due to its strong electrostatic repulsion, other five ligands situate in the identical position and form stable hydrogen bonds network with the riboswitch.

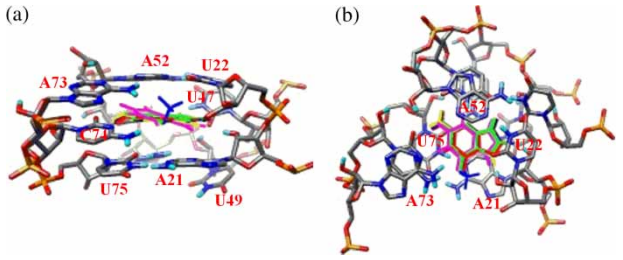


Figure 10. Superimposition of six ligands interacting with residues within 5 Å. (a) Side view; (b) top view. Stick model is for residues and wire for ligands. For ligands, red for ATP, yellow for DZGu, green for HPA, blue for OMGu, magenta for Uric and cyan for guanine (colour online).

### *3.2 Molecular dynamics simulations*

To explore the stabilities and dynamics characteristics of the riboswitch complexes with these ligands, we carried out 10 ns MD simulations based on the docking conformations by using GROMACS program of version 4.0.2 [32], and selected guanine, HPA, Uric and 8MGu as the representatives.

Figure 11 gives the time dependence of RMSDs of riboswitch complexes with the four ligands. The time courses of the distance between the centroid of ligands and U51 as well as C74 are shown in Figure 12.

Figure 11(a) shows that the RMSDs of guanine relative to riboswitch and riboswitch relative to itself approach equilibrium at 4 ns. The RMSD values at the beginning 4 ns show great fluctuations, suggesting remarkable conformational changes. After 4 ns, the system approaches equilibrium with the two RMSD values maintained at 1.8 and 3.2 Å, respectively. In Figure 12(a), the distances of guanine with U51 and C74 are stabilised at 8.25 and 8.50 Å. Because guanine forms three hydrogen bonds with U51 and C74, and one hydrogen bond with U22, these hydrogen bonds restrict the movement of the ligand and, therefore, the position and orientation of ligand are stable during the whole MD simulations.

From Figure 11(b), we can see that the RMSD values of HPA relative to riboswitch and riboswitch relative to itself are basically stabilised at 2.5 and 3.2 Å after 6 ns. But the distance between the centroids of HPA and C74 keeps decreasing slowly, as shown in Figure 12(b), which indicates that the interactions between the ligand and C74 are enhanced gradually. At the same time, the distance between HPA and U51 corresponds to a large fluctuation. Figure 11(a) and (b) reveal that the distances between guanine and the two bases are less than those of HPA, implying that the amino group at 2-position is important for the binding of the ligand.

The RMSDs of Uric relative to riboswitch and riboswitch relative to itself are shown in Figure 11(c). The RMSD values show great fluctuation during the whole simulation. It is probably due to the strong electrostatic repulsion of carbonyl at 2-position of Uric and carbonyl of U51 and C74, which makes the binding of the ligand unstable. In Figure 12(c), the distance between Uric and U51 increases gradually before 8 ns and then decreases slightly, and it is larger than the distance between Uric and C74. In contrast to Figure 12(a), (b) and (d), the distances between Uric and two bases are larger than those of other three ligands. It is probably due to the electrostatic repulsion of hydrogen atom and carbonyl between Uric and U51 that make Uric being far away from two bases.

Figure 11(d) gives the RMSDs of 8MGu. During the simulations, the RMSD of 8MGu relative to the riboswitch is stabilised at 1.8 Å, and that of the riboswitch relative to itself is maintained at 3.0 Å, suggesting a stable binding of

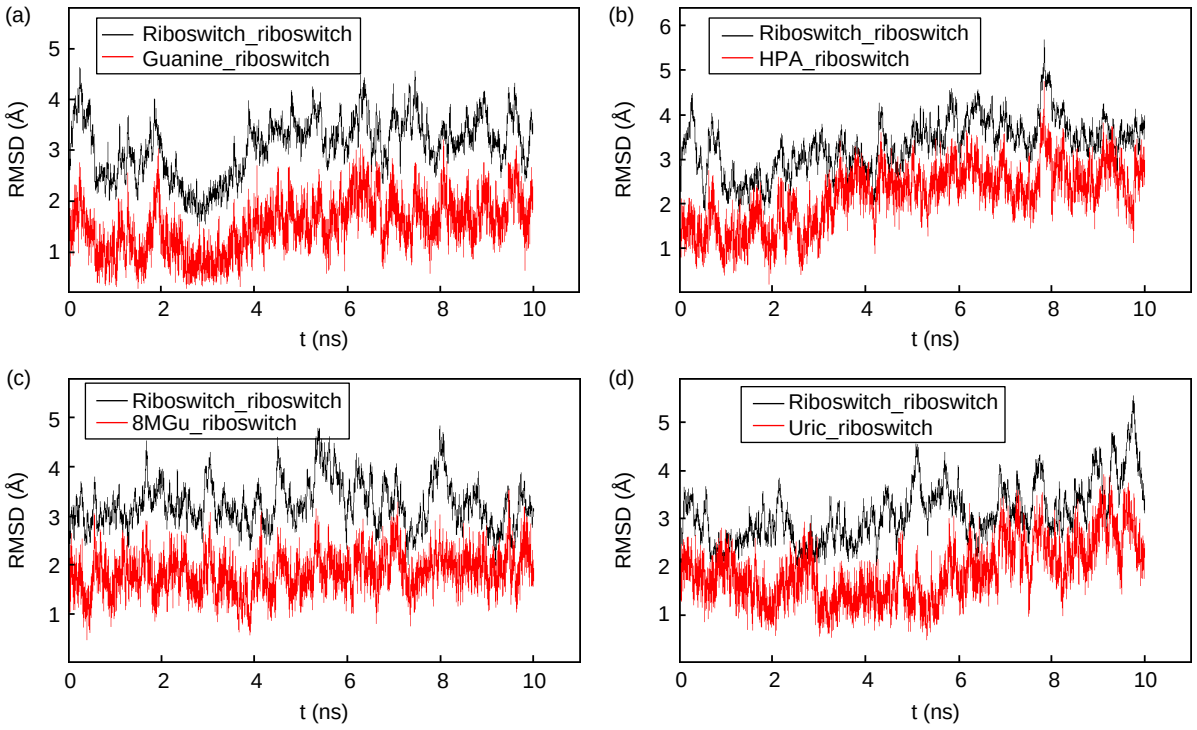


Figure 11. Time dependence of RMSDs. (a) Guanine; (b) HPA; (c) Uric and (d) 8MGu.



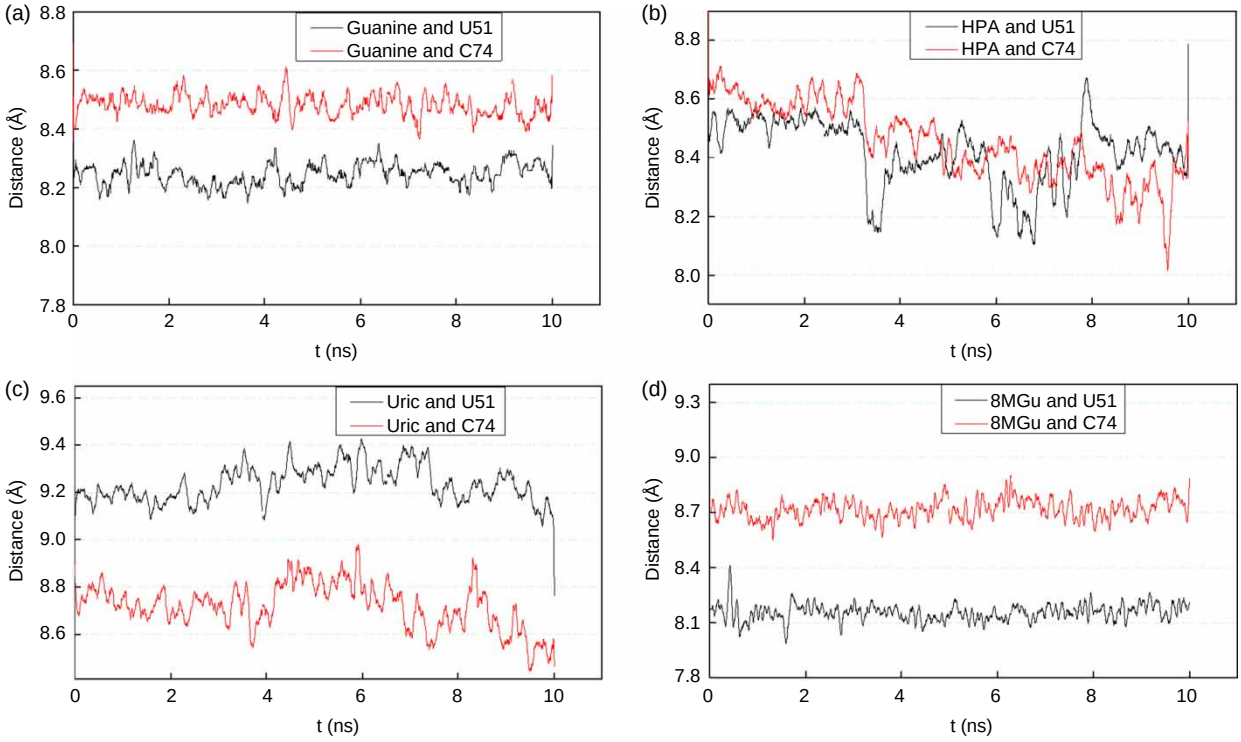


Figure 12. The distance between the centroids of ligands and U51 (black) or C74 (red). (a) Guanine; (b) HPA; (c) Uric and (d) 8MGu (colour online).

8MGu with the riboswitch. Although the binding affinity is weakened due to steric hindrance of methyl, the relative position between 8MGu and riboswitch is very stable. As shown in Figure 12(d), the distances of 8MGu with U51 and C74 are always kept at 8.1 and 8.7 Å, respectively.

The results of MD simulations show that the stabilities of the complexes correlates well with the functional groups of ligands. The binding affinity would change greatly when the structures and functional groups on the ligands are altered.

## 4. Conclusions

Molecular docking and MD simulations were performed on guanine riboswitch and guanine analogues. Our calculations further verified Mandal's experiments [15], i.e. guanine riboswitch can not only bind guanine with high affinity, but also bind its analogues with different affinities. The binding affinity estimated from our calculation is basically consistent with Mandal's experimental results [15]. The orientations of most guanine analogues in the binding pocket are almost identical and are less affected by their functional groups. However, these ligands show different binding affinities. The decreases of the binding affinities are mainly due to the disruptions and weakness of the hydrogen bonds. The hydrogen bonds with U51 and C74 are responsible for molecular recognition.



## Acknowledgements

This work was supported by National Science Foundation of Shandong province (Grant No. ZR2009BM005).

## References

[1] R.T. Batey, *Structures of regulatory elements in mRNAs*, Curr. Opin. Struct. Biol. 16 (2006), pp. 299–306.
[2] M. Mandal and R.R. Breaker, *Gene regulation by riboswitches*, Nat. Rev. Mol. Cell Biol. 5 (2004), pp. 451–463.
[3] W.C. Winkler and R.R. Breaker, *Genetic control by metabolite-binding riboswitches*, Chem. Bio. Chem. 4 (2003), pp. 1024–1032.
[4] A. Serganov, L. Huang, and D.J. Patel, *Structural insights into amino acid binding and gene control by a lysine riboswitch*, Nature 455 (2008), pp. 1263–1268.
[5] M. Mandal, M. Lee, J.E. Barrick, Z. Weinberg, G.M. Emilsson, W.L. Ruzzo, and R.R. Breaker, *A glycine-dependent riboswitch that uses cooperative binding to control gene expression*, Science 306 (2004), pp. 275–279.
[6] W. Winkler, A. Nahvi, and R.R. Breaker, *Thiamine derivatives bind messenger RNAs directly to regulate bacterial gene expression*, Nature 419 (2002), pp. 952–956.
[7] C.D. Stoddard, S.D. Gilbert, and R.T. Batey, *Ligand-dependent folding of the three-way junction in the purine riboswitch*, RNA 14 (2008), pp. 675–684.
[8] S.D. Gilbert, C.D. Stoddard, S.J. Wise, and R.T. Batey, *Thermodynamic and kinetic characterization of ligand binding to the purine riboswitch aptamer domain*, J. Mol. Biol. 359 (2006), pp. 754–768.
[9] S. Brantl, *Metal sensing by RNA in bacteria: Exception or rule?* ACS Chem. Biol. 2 (2007), pp. 656–660.
[10] J.N. Kim and R.R. Breaker, *Purine sensing by riboswitches*, Biol. Cell 100 (2008), pp. 1–11.
[11] A.L. Edwards and R.T. Batey, *A structural basis for the recognition of 2′-deoxyguanosine by the purine riboswitch*, J. Mol. Biol. 385 (2009), pp. 938–948.
[12] S.D. Gilbert, S.J. Mediatore, and R.T. Batey, *Modified pyrimidine specifically bind the purine riboswitch*, J. Am. Chem. Soc. 128 (2006), pp. 14214–14215.
[13] S.D. Gilbert, C.E. Love, A.L. Edwards, and R.T. Batey, *Mutational analysis of the purine riboswitch aptamer domain*, Biochemistry 46 (2007), pp. 13297–13309.
[14] J. Mulhbacher and D.A. Lafontaine, *Ligand recognition determinants of guanine riboswitches*, Nucleic Acids Res. 35 (2007), pp. 5568–5580.
[15] M. Mandal, B. Boese, J.E. Barrick, W.C. Winkler, and R.R. Breaker, *Riboswitches control fundamental biochemical pathways in* bacillus subtilis *and other bacteria*, Cell 113 (2003), pp. 577–586.
[16] F. Khalili-Araghi, J. Gumbart, P.C. Wen, M. Sotomayor, E. Tajkhorshid, and K. Schulten, *Molecular dynamics simulations of membrane channels and transporters*, Curr. Opin. Struct. Biol. 19 (2009), pp. 128–137.
[17] J.L. Klepeis, K. Lindorff-Larsen, R.O. Dror, and D.E. Shaw, *Long-timescale molecular dynamics simulations of protein structure and function*, Curr. Opin. Struct. Biol. 19 (2009), pp. 120–127.
[18] H. Alonso, A.A. Bliznyuk, and J.E. Gready, *Combining docking and molecular dynamics simulations in drug design*, Med. Res. Rev. 26 (2006), pp. 531–568.
[19] Y. Hashem and P. Auffinger, *A short guide for molecular dynamics simulations of RNA systems*, Methods 47 (2009), pp. 187–197.
[20] M. Sharma, G. Bulusu, and A. Mitra, *MD simulations of ligand-bound and ligand-free aptamer: Molecular level insights into the binding and switching mechanism of the add A-riboswitch*, RNA 15 (2009), pp. 1673–1692.
[21] A. Villa, J. Wöhnert, and G. Stock, *Molecular dynamics simulation study of the binding of purine bases to the aptamer domain of the guanine sensing riboswitch*, Nucleic Acids Res. 37 (2009), pp. 4774–4786.
[22] B. Ling, Z. Wang, R. Zhang, X. Meng, Y. Liu, C. Zhang, and C. Liu, *Theoretical studies on the interaction of modified pyrimidines and purines with purine riboswitch*, J. Mol. Graph. Model. 28 (2009), pp. 37–45.
[23] M.J. Frisch, G.W. Trucks, H.B. Schlegel, G.E. Scuseria, M.A. Robb, J.R. Cheeseman, J.A. Montgomery, Jr., T. Vreven, K.N. Kudin, J.C. Burant, J.M. Millam, S.S. Iyengar, J. Tomasi, V. Barone, B. Mennucci, M. Cossi, G. Scalmani, N. Rega, G.A. Petersson, H. Nakatsuji, M. Hada, M. Ehara, K. Toyota, R. Fukuda, J. Hasegawa, M. Ishida, T. Nakajima, Y. Honda, O. Kitao, H. Nakai, M. Klene, X. Li, J.E. Knox, H.P. Hratchian, J.B. Cross, V. Bakken, C. Adamo, J. Jaramillo, R. Gomperts, R.E. Stratmann, O. Yazyev, A.J. Austin, R. Cammi, C. Pomelli, J.W. Ochterski, P.Y. Ayala, K. Morokuma, G.A. Voth, P. Salvador, J.J. Dannenberg, V.G. Zakrzewski, S. Dapprich, A.D. Daniels, M.C. Strain, O. Farkas, D.K. Malick, A.D. Rabuck, K. Raghavachari, J.B. Foresman, J.V. Ortiz, Q. Cui, A.G. Baboul, S. Clifford, J. Cioslowski, B.B. Stefanov, G. Liu, A. Liashenko, P. Piskorz, I. Komaromi, R.L. Martin, D.J. Fox, T. Keith, M.A. Al-Laham, C.Y. Peng, A. Nanayakkara, M. Challacombe, P.M.W. Gill, B. Johnson, W. Chen, M.W. Wong, C. Gonzalez, and J.A. Pople, *Gaussian 03*, *Revision C. 02*, Gaussian, Inc., Wallingford, CT, 2004.
[24] G.M. Morris, D.S. Goodsell, R.S. Halliday, R. Huey, W.E. Hart, R.K. Belew, and A.J. Olson, *Automated docking using a Lamarckian genetic algorithm and an empirical binding free energy function*, J. Comput. Chem. 19 (1998), pp. 1639–1662.
[25] C. Guilbert and T.L. James, *Docking to RNA via root-mean-square-deviation-driven energy minimization with flexible ligands and flexible targets*, J. Chem. Inf. Model. 48 (2008), pp. 1257–1268.
[26] P.A. Holt, J.B. Chaires, and J.O. Trent, *Molecular docking of intercalators and groove-binders to nucleic acids using autodock and surflex*, J. Chem. Inf. Model. 48 (2008), pp. 1602–1615.
[27] N. Moitessier, E. Westhof, and S. Hanessian, *Docking of aminoglycosides to hydrated and flexible RNA*, J. Med. Chem. 49 (2006), pp. 1023–1033.
[28] Z. Yan, S. Sikri, D.L. Beveridge, and A.M. Baranger, *Identification of an aminoacridine derivative that binds to RNA tetraloops*, J. Med. Chem. 50 (2007), pp. 4096–4104.

[29] D. Chen, G. Menche, T.D. Power, L. Sower, J.W. Peterson, and C.H. Schein, *Accounting for ligand-bound metal ions in docking small molecules on adenylyl cyclase toxins*, Proteins 67 (2007), pp. 593–605.
[30] R. Huey, G.M. Morris, A.J. Olson, and D.S. Goodsell, *Software news and update a semiempirical free energy force field with charge-based desolvation*, J. Comput. Chem. 28 (2007), pp. 1145–1152.
[31] R. Odžak, M. Čalić, T. Hrenar, I. Primožič, and Z. Kovarik, *Evaluation of monoquaternary pyrimidium oximes potency to reactive tabun-inhibited human acetylcholinesterase*, Toxicology 233 (2007), pp. 85–96.
[32] D. Van Der Spoel, E. Lindahl, B. Hess, G. Groenhof, A.E. Mark, and H.J.C. Berendsen, *GROMACS: Fast, flexible and free*, J. Comput. Chem. 26 (2005), pp. 1701–1718.
[33] J. Wang, P. Cieplak, and P.A. Kollman, *How well does a restrained electrostatic potential (RESP) model perform in calculating conformational energies of organic and biological molecules?* J. Comput. Chem. 21 (2000), pp. 1049–1074.
[34] J. Wang, W. Wang, P.A. Kollman, and D.A. Case, *Automatic atom type and bond type perception in molecular mechanical calculations*, J. Mol. Graph. Model. 25 (2006), pp. 247–260.
[35] J. Wang, R.M. Wolf, J.W. Caldwell, P.A. Kollman, and D.A. Case, *Development and testing of a general amber force field*, J. Comput. Chem. 25 (2004), pp. 1157–1174.
[36] D.L. Mobley, J.D. Chodera, and K.A. Dill, *On the use of orientational restraints and symmetry corrections in alchemical free energy calculations*, J. Chem. Phys. 125 (2006), 084902.
[37] M. Berrera, S. Pantano, and P. Carloni, *Catabolite activator protein in aqueous solution: A molecular simulation study*, J. Phys. Chem. B 111 (2007), pp. 1496–1501.
[38] E.F. Pettersen, T.D. Goddard, C.C. Huang, G.S. Couch, D.M. Greenblatt, E.C. Meng, and T.E. Ferrin, *UCSF chimera – A visualization system for exploratory research and analysis*, J. Comput. Chem. 25 (2004), pp. 1605–1612.
[39] R.T. Batey, S.D. Gilbert, and R.K. Montange, *Structure of a natural guanine-responsive riboswitch complexed with the metabolite hypoxanthine*, Nature 432 (2004), pp. 411–415.
[40] J.N. Kim, A. Roth, and R.R. Breaker, *Guanine riboswitch variants from mesoplasma florum selectively recognize 2′-deoxyguanosine*, Proc. Natl Acad. Sci. USA 104 (2007), pp. 16092–16097.
[41] S.D. Gilbert, F.E. Reyes, A.L. Edward, and R.T. Batey, *Adaptive ligand binding by the purine riboswitch in the recognition of guanine and adenine analogs*, Structure 17 (2009), pp. 857–868.